arXiv:cond-mat/0303201v2 [cond-mat.dis-nn] 5 Aug 2003

Random Antiferromagnetic Spin-1/2 Chains with Competing Interactions

Eddy Yusuf and Kun Yang
National High Magnetic Field Laboratory and Department of Physics, Florida State University, Tallahassee, Florida 32306

(Dated: February 2, 2008)

We study disordered antiferromagnetic spin-1/2 chains with nearest- and further-neighbor interactions using the real-space renormalization-group method. We find that the system supports two different phases, depending on the ratio of the strength between nearest-neighbor and further-neighbor interactions as well the bond randomness strength. For weak further neighbor coupling the system is in the familiar random singlet phase, while stronger further neighbor coupling drives the system to a large spin phase similar to that found in the study of random antiferromagnetic-ferromagnetic spin chains. The appearance of the large spin phase in the absence of ferromagnetic coupling is due to the frustration introduced by further neighboring couplings, and is unique to the disordered chains.

PACS numbers: 75.10.Jm, 75.10.Nr

I. INTRODUCTION

One-dimensional (1D) quantum spin systems have been of interest to physicists for many years. This is not only because these systems have been good testing grounds for various theoretical techniques and approximations but also because they exhibit a wealth of fascinating low-energy physics. Among various intriguing phenomena of these systems, the interplay between quantum fluctuation and disorder has attracted considerable recent attention. The most thoroughly studied model in this context is the random antiferromagnetic (AF) spin-1/2 chain with nearest neighbor interaction. It has been shown,[1] using the celebrated real space renormalization group (RSRG) method,[2,3] that the low-energy physics of the model is controlled by the random singlet (RS) fixed point of the RSRG and is universal. Among the universal properties of the random singlet phase are the uniform spin susceptibility: $\chi \sim 1/T \log^2 T$, and the disorder averaged spin-spin correlation function: $\langle \mathbf{S}_i \cdot \mathbf{S}_j \rangle \sim (-1)^{i-j}/(i-j)^2$. The RSRG method (with proper extensions) has also been applied with considerable success to a number of other disordered spin chain models (all with nearest neighbor interaction only),[4,5,6,7,8,9,10,11,12,13] as well as two-leg spin ladders.[14,15,16]

In the present work we study random AF spin-1/2 chains with nearest *and* further neighbor couplings, using the RSRG method. Our motivation comes from the following considerations. First of all, as mentioned above, existing theoretical studies have been focusing on models with nearest neighbor couplings only; the RG flow equations of the couplings are relatively simple in this case which allows, for example, exact analytical solution of the fixed point in the case of random AF spin-1/2 chain.[1] In real physical systems, on the other hand, further neighbor couplings are always present, and in certain cases they can even be quite strong. There are a few promising experimental realizations of materials that exhibit non trivial next-nearest neighbor interactions. One of the examples of real physical systems that may meet the criteria is $CuGeO_3$.[17,18,19,20,21] Studies on this system have revealed that the angle of Cu-O-Cu bond is close to 90°. This will induce a competition between antiferromagnetic superexchange between the Cu ions mediated by the oxygen ion and ferromagnetic direct exchange between the Cu ions. As a result the nearest-neighbor superexchange interaction is weakened and hence it is expected that the next-nearest-neighbor interactions which arise from the Cu-O-O-Cu path cannot be neglected. The strength of the second-neighbor bonds can also be controlled by applying pressure to such systems. Masuda and coworker[22] studied the effect of pressure on highly Mg-doped $CuGeO_3$ and found that the frustration is enhanced as the pressure is increased. Another example of material that exhibits non trivial second-neighbor interaction is $Cu_6Ge_6\ O_{18} - xH_2O$ studied by Hase and coworker.[23] Motivated by these experimental realizations, we would thus like to study the effects of next-nearest-neighbor interactions, and in particular, the stability of the RS fixed point against their presence.

Secondly, nearest neighbor models have no frustration in them. Further neighbor interactions, on the other hand, can introduce frustration, and this is known to lead to new physics and phases in the case of pure chains. For example, it is known in the case of spin-1/2 chain with nearest and next nearest neighbor couplings (J_1 and J_2), there are two different phases depending on the ratio between the two.[24,25,26,27,28] For zero or small J_2/J_1, the system is in a gapless (critical) phase with power-law spin-spin correlation, while for larger J_2/J_1 the system spontaneously dimerizes and opens a gap in the excitation spectrum, and the spin-spin correlation becomes short-ranged. In the special case of $J_2/J_1 = 1/2$, which is the so-called Majumdar-Ghosh model, the ground state of the system is known exactly; they are collections of neighboring spins forming singlet pairs over either even or odd nearest neighbor bonds.[29,30,31,32] It is thus of interest to study how frustration affects the physics of disordered chains, and whether new phases can be stabilized by it.

Our results can be summarized as follows. We find that there are two phases in the model we are considering, controlled by the ratio of the strength of nearest-neighbor and next-nearest neighbor interactions and the strength of bond randomness. The Random Singlet (RS) phase is found to be stable against weak further neighbor couplings; in this case the strength of further neighbor couplings (as measured by strength of nearest neighbor couplings) flow to zero as energy scale decreases, thus the low-temperature properties of the system is still controlled by the Random Singlet (RS) fixed point. For strong enough further neighbor couplings, on the other hand, the RS phase becomes unstable and the system is driven into another phase which is controlled by large effective spins at low energies. We find that in this phase the system is still dominated by effective nearest-neighbor interactions at low-energy; however the effective couplings can be either antiferromagnetic or ferromagnetic, with random distributions. We conclude that this phase is the same as that found in random antiferromagnetic (AF)-ferromagnetic (F) spin chain systems with nearest-neighbor interactions only studied by Westerberg *et al.*.[5] The physical origin of the appearance of effective ferromagnetic couplings is the frustration introduced by further neighbor couplings.

The remainder of the paper is organized as follows. In Sec. II we introduce the model we study and discuss the application of RSRG to this model. Results of our numerical studies on the model are presented in Sec. III. In Sec. IV we summarize our findings and make contact with previous works that are related to our studies.

II. THE MODEL

We consider the antiferromagnetic (AF) spin-1/2 chain described by the following Hamiltonian :

$$H = \sum_{i=1}^{N-1} J_i \boldsymbol{S}_i \cdot \boldsymbol{S}_{i+1} + \sum_{i=1}^{N-2} K_i \boldsymbol{S}_i \cdot \boldsymbol{S}_{i+2}, \qquad (1)$$

where N is the number of spins on the chain, $\boldsymbol{S}_i$ is a spin-1/2 operator at the i^{th} site and the positive couplings J_i and K_i are distributed randomly according to some probability distributions which will be described in more details in the next section. The Hamiltonian written down in Eq. (1) consists of two terms, where the first term describes nearest-neighbor interactions between the spins and the second term describes next-nearest-neighbor (n.n.n.) interactions. The schematic diagram of the system described by the Hamiltonian (1) is depicted in Fig. 1(a). We will mostly focus on chains with n.n. and n.n.n couplings in this paper; but some results of chains with couplings beyond n.n.n. will also be presented.

We use the real-space renormalization-group method to study the Hamiltonian (1). The application of this method to AF spin-1/2 chain with n.n. couplings only is well known. The basic idea is to isolate the strongest bond in the system, decimate it, and calculate the effective interactions generated between what were the third-nearest neighbors. The key simplifying features in this case are that the generated interactions are always antiferromagnetic, and they connect only nearest-neighbor spins (after the two spins coupled by the strongest bond are removed).

Appropriate extensions of the original RG scheme need to be included in order to study the present model with further neighbor couplings properly. First we notice that the coordination number, i.e. the number of spins coupled to a given spin, grows as the energy scale is lowered so we need to keep track of the structure of the system. This is in contrast to the AF spin-1/2 chain with n.n. couplings where the coordination number is always 2. Second, as we will see later, effective ferromagnetic couplings may be generated at certain stage as RSRG is carried out in the presence of antiferromagnetic n.n.n. couplings. The formation of ferromagnetic couplings allows the possibility of generating effective spins with sizes larger than 1/2, so we need to extend the RG rules to incorporate arbitrary spin sizes and coupling signs. Let us discuss these in more detail. Consider spin 3 and 4 in Fig. 1(a) which are coupled by the strongest bond, and other spins in the system that couple to at least one of them. Due to the presence of n.n.n. couplings, we have a six-spin problem instead of a four-spin problem for a given pair of spins coupled by the strongest bond. The Hamiltonian for the six-spin problem is given by :

$$H = H_0 + H_I, \qquad (2)$$

where

$$\begin{aligned} H_0 &= J_{34} \boldsymbol{S}_3 \cdot \boldsymbol{S}_4, \\ H_I &= J_{23} \boldsymbol{S}_2 \cdot \boldsymbol{S}_3 + J_{45} \boldsymbol{S}_4 \cdot \boldsymbol{S}_5 + J_{13} \boldsymbol{S}_1 \cdot \boldsymbol{S}_3 \\ &+ J_{35} \boldsymbol{S}_3 \cdot \boldsymbol{S}_5 + J_{24} \boldsymbol{S}_2 \cdot \boldsymbol{S}_4 + J_{46} \boldsymbol{S}_4 \cdot \boldsymbol{S}_4, \end{aligned} \qquad (3)$$

where J_{ij} is the antiferromagnetic coupling between $\boldsymbol{S}_i$ and $\boldsymbol{S}_j$. We have shown in our previous work on the spin ladders[15] that to the second order perturbation calculation, H_I only generates pairwise interactions among the spins and hence it is only necessary to include a pair of spins coupled to the two spins connected by the strongest bond when we consider the effective interaction between them, i.e. we just have to consider four-spin clusters for a given segment which contains the strongest bond. Let us consider the most complicated four-spin cluster where a given spin is coupled to three other spins as depicted in Fig. 2. The renormalized coupling between two spins in the cluster, say spins 2 and 5, is given by :

$$\begin{aligned} \tilde{J}_{25} &= J_{25} + \frac{1}{2J_{34}}(J_{23}J_{45} + J_{24}J_{35} - J_{23}J_{35} - J_{24}J_{45}) \\ &= J_{25} + \frac{1}{2J_{34}}(J_{23} - J_{24})(J_{45} - J_{35}) \end{aligned} \qquad (4)$$

where $\tilde{J}_{ij}$ is the *renormalized* coupling between $\boldsymbol{S}_i$ and $\boldsymbol{S}_j$, and J_{ij} is the *original* bond between $\boldsymbol{S}_i$ and $\boldsymbol{S}_j$.

Examining Eq. 4, we can see that some of the contributions to the renormalized coupling from 2nd order processes are *ferromagnetic*. The overall sign of the total interaction between the second and fifth spin will be determined by the relative strength between the antiferromagnetic nearest-neighbor and next-nearest-neighbor bonds. In general if the n.n.n. couplings are very weak compared to the n.n. couplings then the ferromagnetic interactions will not appear. This is quite different from what we found in the study of the ladder where effective ferromagnetic interactions appear as soon as the RG is applied to the system. Due to the possibility of the appearance of ferromagnetic couplings at some step of RG, it is necessary to generalize the RG procedure to include arbitrary spin sizes and coupling signs. The discussion on how this is done has been spelled out in great detail in our earlier work on the spin ladder.[15] We carry out the numerical calculation using the rules described in previous paragraphs and present the results in the next section.

III. NUMERICAL RESULTS

We present numerical results for spin chains with nearest-neighbor (n.n.) and next-nearest-neighbor (n.n.n.) interactions with total number of spins up to 60000. We search for the bond with the largest gap, Δ_0, which is defined as the gap between the ground state and the first excited state, decimate it, and calculate the effective interactions among the remaining spins. The procedure is repeated until the number of spins left is about 1% of the original number of spins in the system. We use 100 samples and take the disorder average over all these samples in all our calculations. The nearest-neighbor bonds are chosen to be distributed randomly according to the power-law probability distribution:

$$P_{n.n.}(J_i) = (1-\alpha)J_i^{-\alpha}, 0 < J_i < 1, \tag{5}$$

where the power-law exponent $\alpha < 1$ parametrizes the randomness strength; the larger α, the stronger the randomness. The reason for choosing a power-law form is because for the random spin-1/2 chain, the fixed point distribution is known to be in the power-law form. So by choosing initial distributions in the power-law form, we expect to start closer to the fixed point and hence reduce the necessity to use larger system size.

We consider two different ways of generating the n.n.n. bonds. First we consider n.n.n. bonds which are completely correlated with the n.n. bonds, where next-nearest-neighbor bond K_i is determined from the n.n. bonds through the following relation:

$$K_i = \Lambda \frac{J_i J_{i+1}}{\Omega_0}, \tag{6}$$

where Λ is a parameter introduced to control the strength of next-nearest-neighbor interactions and Ω_0 is the cutoff of the initial nearest-neighbor bonds distribution, which is 1. In the limit $\Lambda \to 0$, the AF spin-1/2 chain with nearest-neighbor interactions only is recovered. Eq. (6) comes from the following consideration. The interactions between two spins come from the overlap integral of the electron wave functions which are bound to the atoms sitting on the lattice sites. In general, the wave function decays exponentially at large distances, and so does the overlap integral. Let us consider three electrons sitting on different lattice sites labeled 1,2, and 3. For two electrons separated by a distance R, the typical interaction would have a form of $J \sim e^{-R/a}$, where a is a length scale of order the size of the wave function. Based on this picture, the interaction between the first and third spins, which is basically the overlap integral between the first and third spins, can be written as $J \sim e^{-(R_3-R_1)/a}$, where R_3 and R_1 are measured with respect to some reference point. This relation can be rewritten as :

$$J \sim e^{-(R_3-R_2)/a} e^{-(R_2-R_1)/a} \propto J_2 J_1, \tag{7}$$

where J_i is the overlap integral between S_i and S_{i+1}. Hence, it is reasonable to model the correlation as the product of two nearest-neighbor bonds as shown in Eq. (6). We focus mostly on this type of further neighbor coupling, and unless stated otherwise, the results presented below are for this type of further neighbor coupling. For comparison, we have also studied cases in which the n.n.n. couplings are uncorrelated case with the n.n. couplings, i.e. the n.n.n. bonds are distributed randomly in the system, independent of of the distribution of the n.n. bonds. We choose the distribution to be in a power-law form with the same exponent, but a different cutoff Λ :

$$P_{n.n.n.}(K_i) = \frac{1-\alpha}{\Lambda^{1-\alpha}} K_i^{-\alpha}, 0 < K_i < \Lambda. \tag{8}$$

Again Λ parametrizes the strength of n.n.n. couplings. As we will see later, while the topology of the phase diagrams are the same for these two cases, there is huge quantitative differences in the position of the phase boundary.

As we carry out RSRG numerically, we monitor the appearance and proliferation of large effective spins in the system. We plot the sample-averaged fraction of spins larger than 1/2 as a function of energy scale, Δ_0, in Fig. 3. The left panel of Fig. 3 shows how the formation of large effective spins evolves as the energy scale, Δ_0, is lowered by fixing $\alpha = 0$ and varying n.n.n. bond strength controlled by Λ, while the right one by fixing $\Lambda = 0.55$ and varying α. Let us analyze the left panel of Fig. 3. It is very clear that, for fixed α, different antiferromagnetic n.n.n. bond strength will lead to different scenarios in the low energy limit. For weak enough Λ (in the regime where $\Lambda < 0.5$) we do not find spin sizes other than 1/2; not only we never find any spin larger than 1/2 but also we never find any ferromagnetic bonds in this regime. The situation drastically changes when we tune the strength of antiferromagnetic n.n.n. bonds up to 0.55

where we can see clearly that large effective spins dominate in the low energy limit and drive the system into a new phase. This can be understood in the following way. For weak enough n.n.n. bonds, these interactions are always suppressed by the presence of n.n. bonds. We have explained in Eq. (4) that the ferromagnetic bond will appear if the n.n.n. bonds are strong enough to overcome the n.n. bonds. Apparently for $\Lambda < 0.5$, the n.n.n. bonds are too weak to compete with n.n. bonds so we never see the emergence of ferromagnetic interactions in the system. On the other hand, for $\Lambda > 0.55$, the antiferromagnetic n.n.n. bonds are strong enough to overcome the n.n. bonds and allow the appearance of ferromagnetic bonds which in turn will drive the system into a new phase controlled by large effective spins.

The right panel of Fig. 3 shows another study of how large effective spins appear in the system by varying the disorder strength α for fixed $\Lambda = 0.55$. We find that the formation of large effective spins is suppressed as the bond disorder gets stronger. This also has a simple explanation. With increasing bond disorder strength, the probability of finding weak n.n. bonds is getting bigger. This will give us even weaker n.n.n. bonds because of the correlation between a next-nearest-neighbor bond with two nearest-neighbor bonds as given by Eq. 6. These weak n.n.n. bonds can not compete with the n.n. bonds which in turn will suppress the formation of ferromagnetic bonds in the system. Based on this view, we can understand why large effective spins are more difficult to form in the regime where the bond disorder is strong. So for strong enough bond disorder, no ferromagnetic bonds will appear due to the fact that n.n.n. bonds could not compete with n.n. bonds and the system will remain in the Random Singlet (RS) phase.

The appearance of a new phase can also be deduced from plotting the sample-averaged χT as a function of temperature where the temperature is associated with the energy scale, Δ_0. We plot this in Fig. 4 where in the left panel α is fixed and Λ is varied, whereas in the right panel Λ is fixed and α is varied. χT in the RS phase is well known to be given by $1/log^2 T$. For fixed $\alpha = 0$, we can see increasing deviations from $1/log^2 T$ with increasing strength for Λ which gives us a clear indication that the system is driven away from the RS phase; for $\lambda > 0.5$ instead of falling as $1/log^2 T$, χT appears to approach a constant in the low-T limit. The explanation for this behavior is similar to the discussion in the previous paragraph. Strong enough n.n.n. bonds will allow the appearance of ferromagnetic bonds which in turn will form large effective spins in the low energy limit. These strongly correlated effective spins govern the susceptibility of the system at low temperature. The susceptibility in this phase has different origin from the susceptibility for the RS phase where the contribution comes from the undecimated half spins. The same situation is encountered when Λ is fixed and α is varied as shown on the right panel of Fig. 4. The deviations are more significant for small α. This is consistent with our discussion on the previous paragraph that for strong enough bond disorder, the system will remain in the RS phase because the overall strength of n.n.n. bonds is much weaker than that of n.n. bonds. This is indeed what we see in our numerical results that χT for bigger $\alpha(> 0.6)$ is closer to the value for RS phase $1/log^2 T$.

We have established that there two phases in the system. The transition from one phase to another is controlled by the strength of bond disorder α and the strength of n.n.n. bonds Λ. For $\alpha = 0$ and $\Lambda < 0.5$ the system remains in the RS phase while for $\Lambda > 0.55$ the system is driven into the new phase. We have already seen that the new phase is controlled by large effective spins in the low energy limit. Is there any other parameter we can use to study the nature of of the new phase? We address this question by studying the ratio of n.n. bond strength to n.n.n. bond strength in the two phases as shown in Fig. 5. It is found that on either side of the phase boundary, nearest-neighbor bonds always dominate further-neighbor bonds.[33] Now we have a more complete picture of the new phase found in the system. The new phase is controlled by large effective spins in the low energy limit and the dominant interactions come from the nearest-neighbor bonds only. These nearest-neighbor interactions consist of both antiferromagnetic and ferromagnetic bonds. These results suggest that in the low energy limit, spin chains with antiferromagnetic n.n. and sufficiently strong n.n.n. interactions behave just like random antiferromagnetic-ferromagnetic spin chains, including a Curie susceptibility discussed earlier. This brings us to the conclusion that the new phase found in the system we are studying is the same as the large spin phase found in the random antiferromagnetic-ferromagnetic spin chains in the low energy limit. The numerically determined phase diagram for spin chains with random antiferromagnetic n.n. and n.n.n. bonds is shown in Fig. 6.

The left panel of this figure shows the phase diagram for the correlated next-nearest-neighbor bonds as given by Eq. (6) whereas the right panel for uncorrelated next-nearest-neighbor bonds. In both cases we find that the system supports only two phases, which are the Random Singlet phase and the Large Spin phase. There are some differences of the phase boundaries on these two cases. First, the trend on how the phase boundaries change as we vary α and Λ is different for the correlated and uncorrelated next-nearest-neighbor bonds. For the correlated case, Λ stays constant as we increase α from 0 to 0.6 and tends to increase for α larger than 0.6. For the uncorrelated one, Λ decreases with increasing α. Secondly, the magnitude of critical Λ for the uncorrelated n.n.n. couplings is much smaller than that for the correlated case, by as much as 10 orders of magnitude for α close to 1!

We believe the these differences can be understood as the following. For the uncorrelated case we assign a probability distribution function for the n.n.n. bonds whose cutoff is determined by Λ, and the bonds are generated independent of the configuration of the n.n. bonds. Al-

though in general the strength of the n.n.n. bonds is much weaker than that of n.n. bonds when Λ is small, due to the uncorrelated nature of the way they are generated, there is a small probability that the next-nearest-neighbor coupling is actually stronger than the nearest-neighbor ones in some region of the system. As we have explained earlier in the text, the overall sign of the total interaction generated by RG between two spins depends heavily on the relative strength of the antiferromagnetic n.n. and n.n.n. bonds; thus such rare events can lead to the generation of ferromagnetic bonds, which in turn may proliferate as energy scale goes down. In the correlated case, on the other hand, such rare events are greatly suppressed by the correlation between n.n. and n.n.n. bonds. We also know that α parametrizes the width of the distribution; for a given Λ in the uncorrelated case, the bigger α is, the wider the distributions are for both the n.n. and n.n.n. bond distributions, thus the larger the probability of the rare events discussed above are, and the more likely ferromagnetic couplings get generated. On the other hand this effect is again suppressed for the case of correlated n.n.n. bonds, due to the way we parametrizes their strength; the larger α is, the smaller the overall strength of the n.n.n. bonds due to the way the are generated.

As discussed earlier, the appearance of effective ferromagnetic couplings is a consequence of competition between nearest and further neighbor couplings, or frustration. We have also studied spin chains with further-neighbor interactions which do *not* introduce frustration to the system. This can be done by introducing ferromagnetic next-nearest-neighbor bonds or antiferromagnetic third-nearest-neighbor bonds. The ferromagnetic next-nearest-neighbor bonds and antiferromagnetic third-nearest-neighbor bonds are generated in the same way as discussed at the beginning of this section, i.e. the bonds are generated through Eq. (6). We present our results for this particular system in Fig. 7.

The upper panels of Fig. 7 show the sample-averaged plot of the strength of nearest-neighbor interactions compared to the strength of further-neighbor interactions and the fraction of spins with sizes larger than 1/2 as a function of energy scale, Δ_0, for the system with ferromagnetic next-nearest-neighbor bonds. We choose to fix $\alpha = 0$ and to vary Λ to see how the ratio changes as the energy scale is lowered. We find that the nearest-neighbor interactions always dominate over further-neighbor interactions at all energy scale. The evolution of the spin sizes as the energy scale is lowered is also studied here. The result shows that no spin having sizes larger than 1/2 is found in the system. Based on these results we conclude that the presence of ferromagnetic next-nearest-neighbor bonds does not drive the system into a new phase. The couplings are dominated by antiferromagnetic bonds which suppress the formation of effective spins larger than 1/2 at low energy. In the low energy limit the system stays in the RS phase. The lower panels of Fig. 7 show the plot of the ratio between the strength of nearest and further neighbor bonds and the fraction of spins with sizes larger than 1/2 as a function of energy scale, Δ_0, for the system with antiferromagnetic third-nearest-neighbor bonds. We also fixed $\alpha = 0$ and vary Λ for this case. The results are the same for those with ferromagnetic next-nearest-neighbor bonds. These results give us a strong indication that the system stays in the RS phase. We can thus conclude that non-frustrating further neighbor bonds act as irrelevant perturbations in the low energy limit, and hence the system stays in the RS phase.

IV. SUMMARY AND DISCUSSION

In this paper we have used the real space renormalization group method to study random antiferromagnetic spin-1/2 chains, with both nearest- and further neighbor interactions. We find that the system supports two phases, the random singlet phase and the large spin phase. The latter is only stabilized by sufficiently strong further neighbor couplings that compete with the nearest neighbor couplings, so that there is frustration in the system.

The real space renormalization group procedure is quantitatively accurate only when the initial distributions of the couplings are broad. We believe, however, our conclusion remains valid even if the initial distribution of couplings is not broad. In the case of nearest neighbor coupling only, Doty and Fisher[34] showed that weak bond randomness is a relevant perturbation that immediately destabilizes the Luttinger liquid fixed point that describes the gapless phase of the pure chain, and bond randomness *grows* as energy scale goes down, eventually brings the system to the random singlet fixed point. Their arguments remain valid even in the presence of further neighbor couplings, as long as they are not strong enough to destabilize the gapless phase in the absence of bond randomness. On the other hand when they are strong enough to put the pure system in the gapped phase with spontaneous dimerization, one of us[35] showed that the dimerized phase is *also unstable* against weak randomness, as randomness nucleates solitons and destroys spontaneous dimerization; the low-energy degrees of freedom are the half-spins carried by the solitons, with random interaction with broad distribution (due to the fluctuation of inter soliton distance etc). Depending on whether the coupling between these spins are purely AF or both F and AF, the systems can be in either one of the two phases we find here. We thus conclude these are the only two phases the system supports in the presence of any amount of bond randomness.[36]

The frustration induced ferromagnetic coupling and the resultant large spin formation has been discussed in a different context before.[10] In that work Yang and Bhatt studied spin-1 chains with random AF nearest neighbor bonds, with both quadratic and bi-quadratic couplings on each bond. It was shown that even though overall

each individual bond is AF, as long as in some of the bonds the quadratic and bi-quadratic couplings have opposite tendency (i.e., one AF and the other F), effective ferromagnetic couplings may be generated at low-energy, and the large spin phase stabilized. In this case the bonds are frustrated due to the competition between quadratic and bi-quadratic couplings on the *same* bond. Thus the phenomena of frustration induced large spin formation, although never seen in pure systems, may actually be rather generic in disordered systems.

Acknowledgments

We have benefited greatly from very useful discussions with R. N. Bhatt. This work was supported by NSF grant No. DMR-0225698, the Center for Materials Research and Technology (MARTECH), and the A. P. Sloan Foundation.

[1] D. S. Fisher, Phys. Rev. B **50**, 3799 (1994).
[2] S. K. Ma, C. Dasgupta and C.-K. Hu, Phys. Rev. Lett. **43**, 1434 (1979); C. Dasgupta and S. K. Ma, Phys. Rev. B **22**, 1305 (1980).
[3] R. N. Bhatt and P. A. Lee, Phys. Rev. Lett. **48**, 344 (1982).
[4] D. S. Fisher, Phys. Rev. Lett. **69**, 534 (1992); Phys. Rev. B **51**, 6411 (1995).
[5] E. Westerberg, A. Furusaki, M. Sigrist, and P. A. Lee, Phys. Rev. Lett. **75**, 4302 (1995); Phys. Rev. B **55**, 12578 (1997).
[6] R. A. Hyman, K. Yang, R. N. Bhatt and S. M. Girvin, Phys. Rev. Lett. **76**, 839 (1996).
[7] B. Boechat, A. Saguia, and M. A. Continentino, Solid State Commun. **98**, 411 (1996); A. Saguia, B. Boechat, and M. A. Continentino, Phys. Rev. B **58**, 58 (1998).
[8] R. A. Hyman and K. Yang, Phys. Rev. Lett. **78**, 1783 (1997).
[9] C. Monthus, O. Golinelli, and Th. Jolicoeur, Phys. Rev. Lett. **79**, 3254 (1997); Phys. Rev. B **58**, 805 (1998).
[10] K. Yang and R. N. Bhatt, Phys. Rev. Lett. **80**, 4562 (1998); Physica B **259**, 1048 (1999); R. N. Bhatt and K. Yang, J. Appl. Phys. **83**, 7231 (1998).
[11] K. Damle, O. Motrunich, and D. A. Huse, Phys. Rev. Lett. **84**, 3434 (2000); O. Motrunich, K. Damle, and D. A. Huse, Phys. Rev. B **63** 134424 (2001); K. Damle, Phys. Rev. B **66**, 104425 (2002).
[12] G. Refael, S. Kehrein, and D. S. Fisher, Phys. Rev. B **66**, 060402 (2002).
[13] A. Saguia, B. Boechat, and M. A. Continentino, Phys. Rev. Lett. **89**, 117202 (2002).
[14] R. Melin, Y.-C. Lin, P. Lajko, H. Rieger, and F. Igloi, Phys. Rev. B **65**, 104415 (2002).
[15] E. Yusuf and K. Yang, Phys. Rev. B **65**, 224428 (2002).
[16] E. Yusuf and K. Yang, Phys. Rev. B **67**, 144409 (2003).
[17] J. E. Lorenzo, K. Hirota, G. Shirane, J. M. Tranquada, M. Hase , K. Uchinokura, H. Kojima, I. Tanaka, and Y. Shibuya, Phys. Rev. B **50**, 1278 (1994).
[18] J. Riera and A. Dobry, Phys. Rev. B **51** 16098 (1995)
[19] G. Castilla, S. Chakravarty, and V. J. Emery, Phys. Rev. Lett. **75**, 1823 (1995).
[20] L. P. Regnault, M. Ain, B. Hennion, G. Dhalenne, and A. Revcolevschi, Phys. Rev. B **53** 5579 (1996).
[21] Y. Mizuno, T. Tohyama, S. Maekawa, T. Osafune, N. Motoyama, H. Eisaki, and S. Uchida, Phys. Rev. B **57** 5326 (1998).
[22] T. Masuda, D. Yano, R. Kuroda, K. Uchinokura, H. Kuroe, T. Sekine, Y. Katsuki, K. Ohwada, Y. Fujii, H. Nakao, and Y. Murakami, Phys. Rev. B **67** 024423 (2003).
[23] Masashi Hase, Kiyoshi Ozawa, and Norio Shinya, cond-mat/0304323.
[24] F. D. M. Haldane, Phys. Rev. B **25**, 4925 (1982); **26**, 5257 (1982).
[25] K. Kuboki and H. Fukuyama, J. Phys. Soc. Japan **56**, 3126 (1987).
[26] T. Tonegawa and I. Harada, J. Phys. Soc. Japan **56**, 2153 (1987).
[27] I. Affleck, D. Gepner, H. J. Schulz, and T. Ziman, J. Phys. A **22**, 511 (1989).
[28] K. Okamoto and K. Nomura, Phys. Lett. A **169**, 433 (1992).
[29] C. K. Majumdar, J. Phys C **3**, 911 (1970).
[30] C. K. Majumdar and D. K. Ghosh, J. Math. Phys. **10**, 1399 (1969).
[31] P. M. can den Broek, Phys. Lett. A **77**, 261 (1980).
[32] B. S. Shastry and B. Sutherland, Phy. Rev. Lett. **47**, 964 (1981).
[33] As RG is applied to the chain, the coordination number grows, and a given spin may couple to many other spins so at this point we divide the interactions into two types: nearest-neighbor bonds and those other than nearest-neighbor bonds, i.e. further-neighbor bonds.
[34] C. A. Doty and D. S. Fisher, Phys. Rev. B **45**, 2167 (1992).
[35] K. Yang, R. A. Hyman, R. N. Bhatt and S. M. Girvin, J. Appl. Phys. **79**, 5096 (1996).
[36] In the present and previous (Ref.35) work we only considered further neighbor coupling up to certain distance. It is possible that there are other phases if there is (power-law) long-range spin coupling (R. N. Bhatt, private communication).

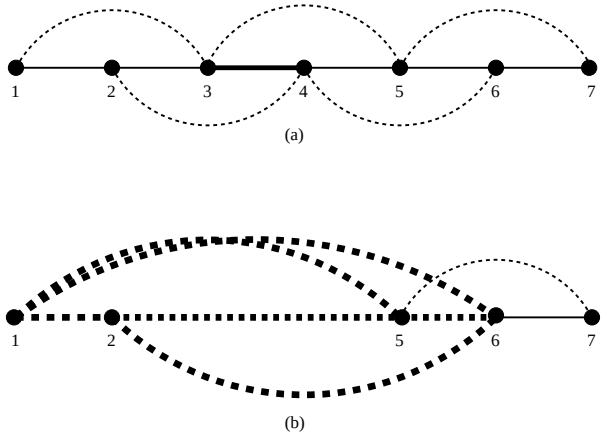

FIG. 1: (a) Schematic diagram for the AF spin-1/2 chain given by the Hamiltonian (1). In addition to the nearest-neighbor couplings between the spins, we also include the next-nearest-neighbor couplings represented by the dashed lines. Here the strongest bond is represented by the thick bold line. (b) The renormalization scheme after the strongest bond is decimated. The thick dashed lines are the renormalized couplings.

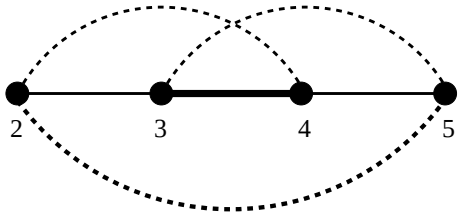

FIG. 2: The most complicated structure of a four-spin cluster where a given spin is coupled to the other three spins.

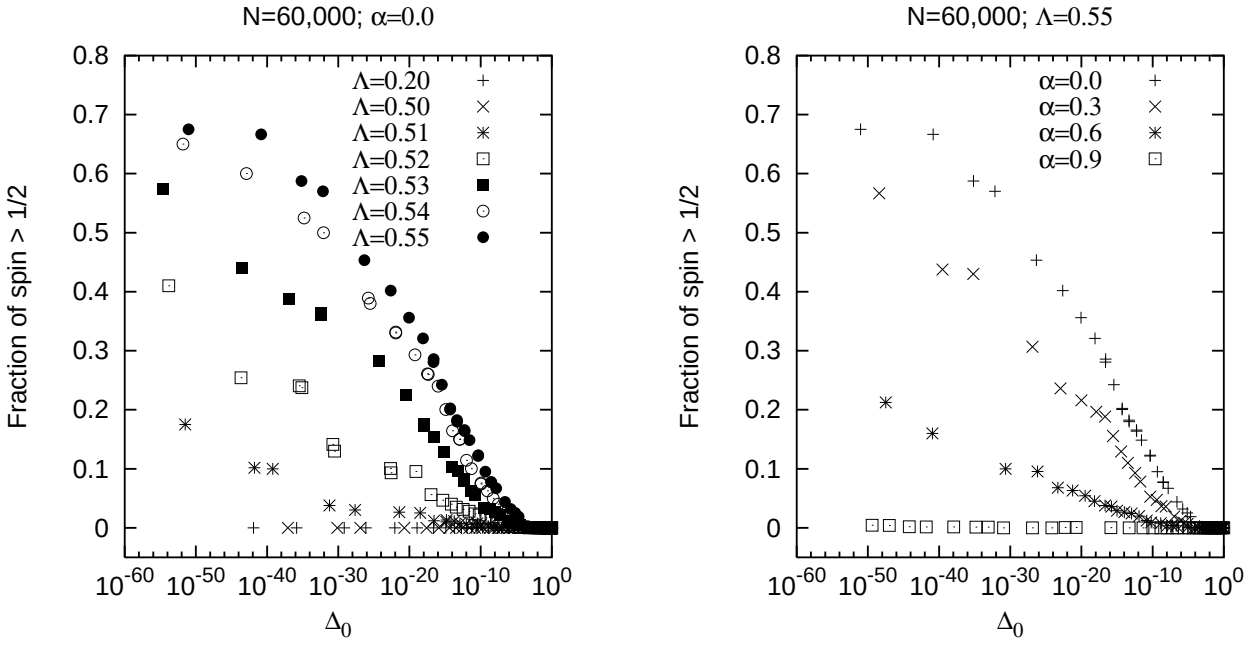

FIG. 3: The sample-averaged fraction of spins larger than 1/2 as a function of energy scale, Δ_0. The error bars are about the size of the data points shown in the figure. The left panel shows how the fraction of spins larger than 1/2 for $\alpha = 0.0$ changes as Λ is varied and the right panel for $\Lambda = 0.55$ as α is varied. Both are calculated for N=60,000. Strong enough next-nearest-neighbor interactions will drive the system into a new phase controlled by large effective spins. All calculations are done with correlated next-nearest-neighbor bonds given in Eq. (6).

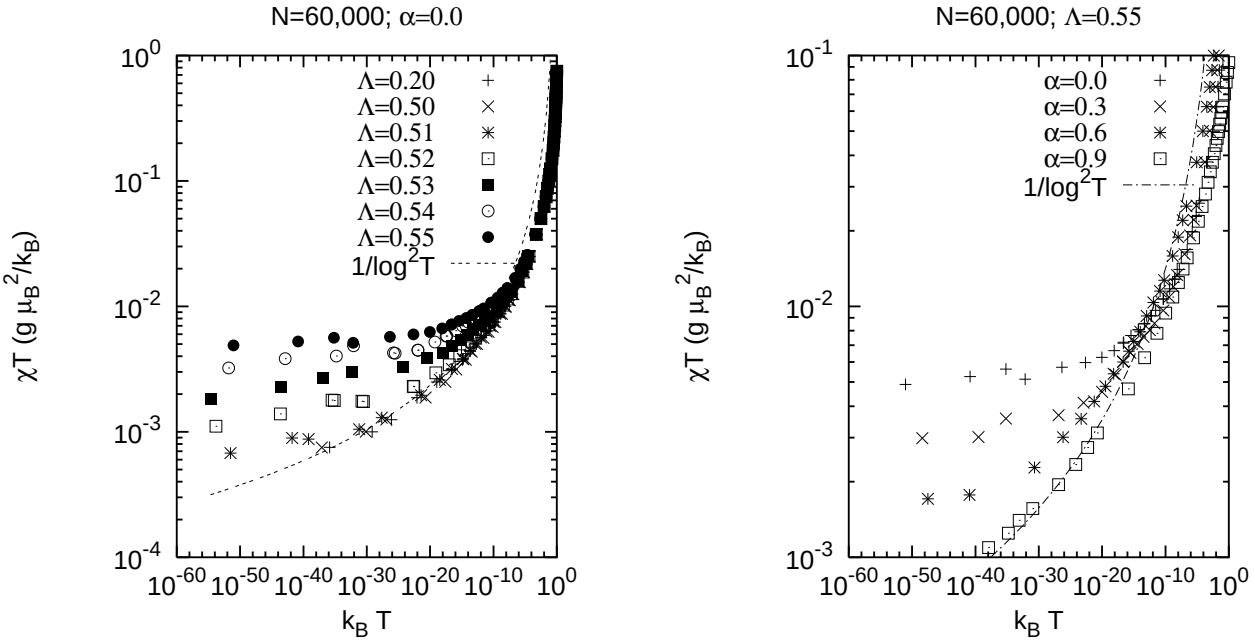

FIG. 4: The sample-averaged χT as a function of parameters of the model, α and Λ. The error bars are about the size of the data points. For strong enough correlated next-nearest-neighbor interactions, given in Eq. (6), the susceptibilities behave differently from $1/Tlog^2T$. The contribution to the susceptibilities come from large effective spins formed at low temperature.

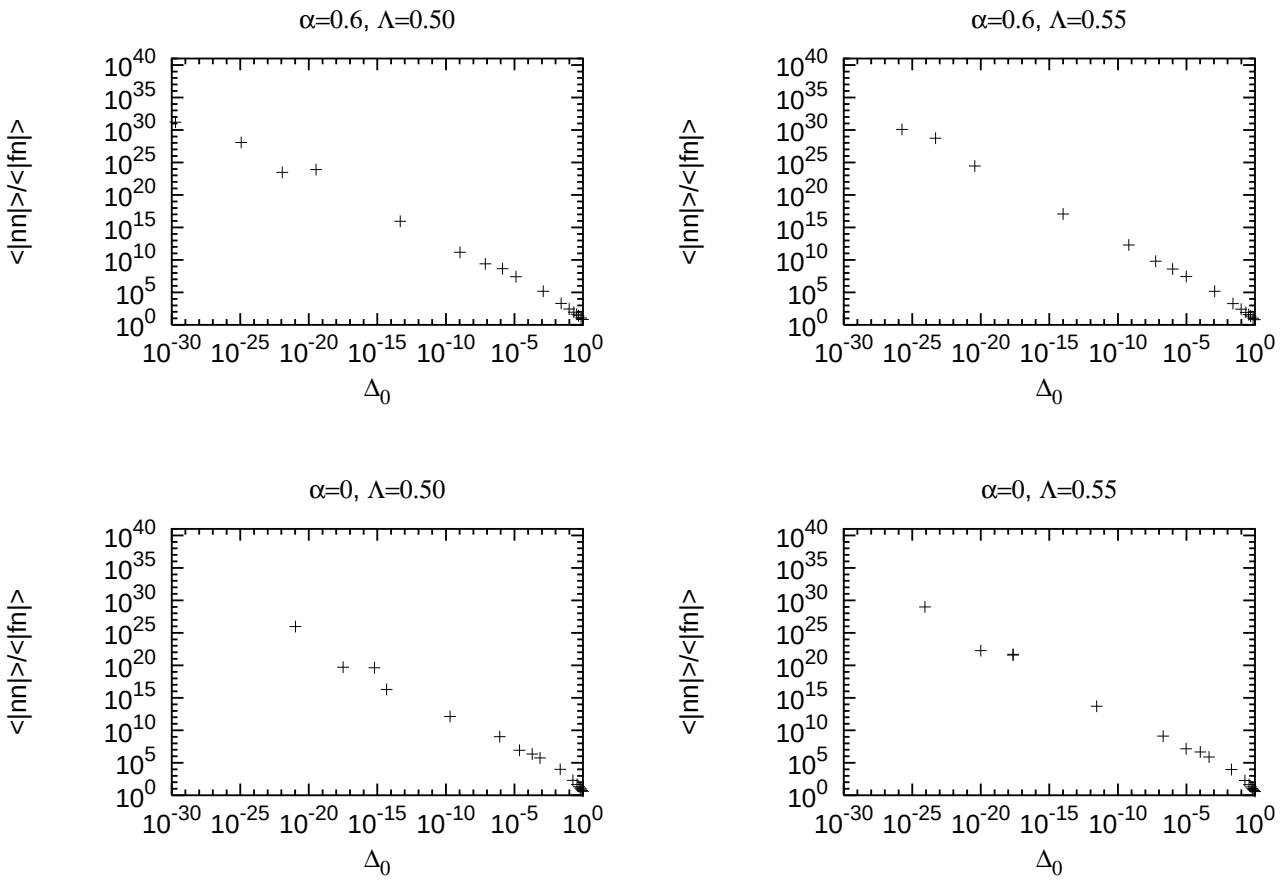

FIG. 5: The sample-averaged ratio of the strength of the nearest-neighbor bonds to the strength of the bonds that are beyond nearest neighbor as a function of energy scale. It is clear from the plot that in either side of the phase, the interactions are dominated by nearest-neighbor bonds only. We use the correlated next-nearest-neighbor interactions defined in Eq. (6).

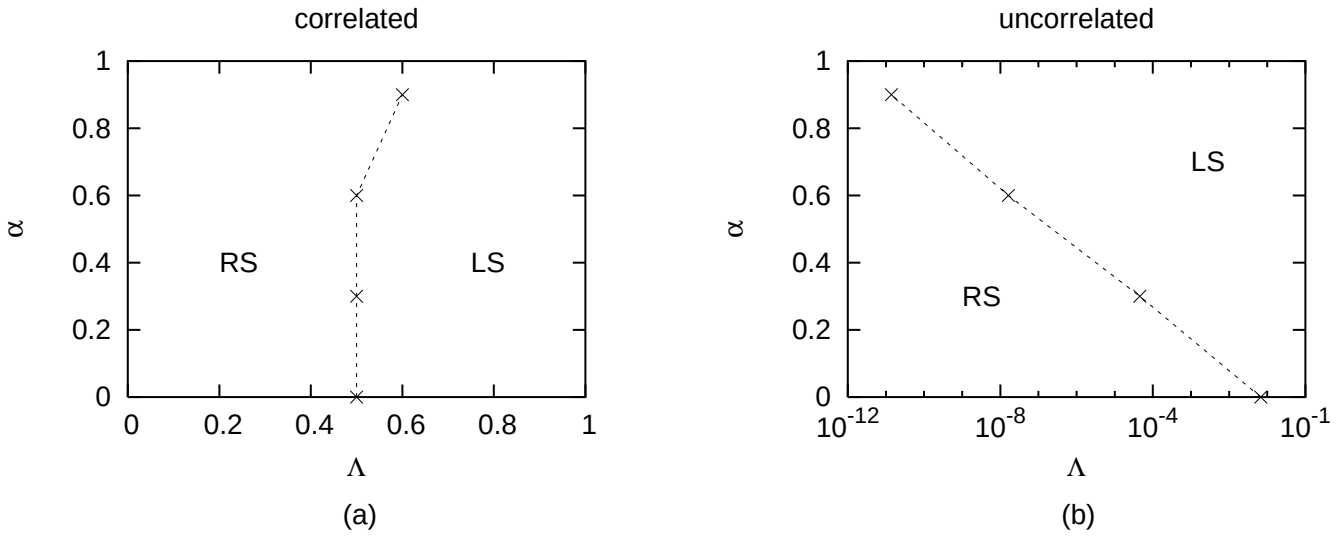

FIG. 6: (a) The numerically determined phase diagram for spin chains with competing interactions between nearest-neighbor and next-nearest-neighbor interactions. The n.n.n. interactions are correlated with the n.n. interactions (see text). (b) The numerically determined phase diagram for spin chains with uncorrelated n.n.n. interactions. In both cases α denotes the strength of the bond randomness and Λ represents the strength of the next-nearest-neighbor interactions. The crosses in both figures are obtained from numerical calculations. The dashed lines are drawn by connecting the data points to see the phase boundary more clearly.

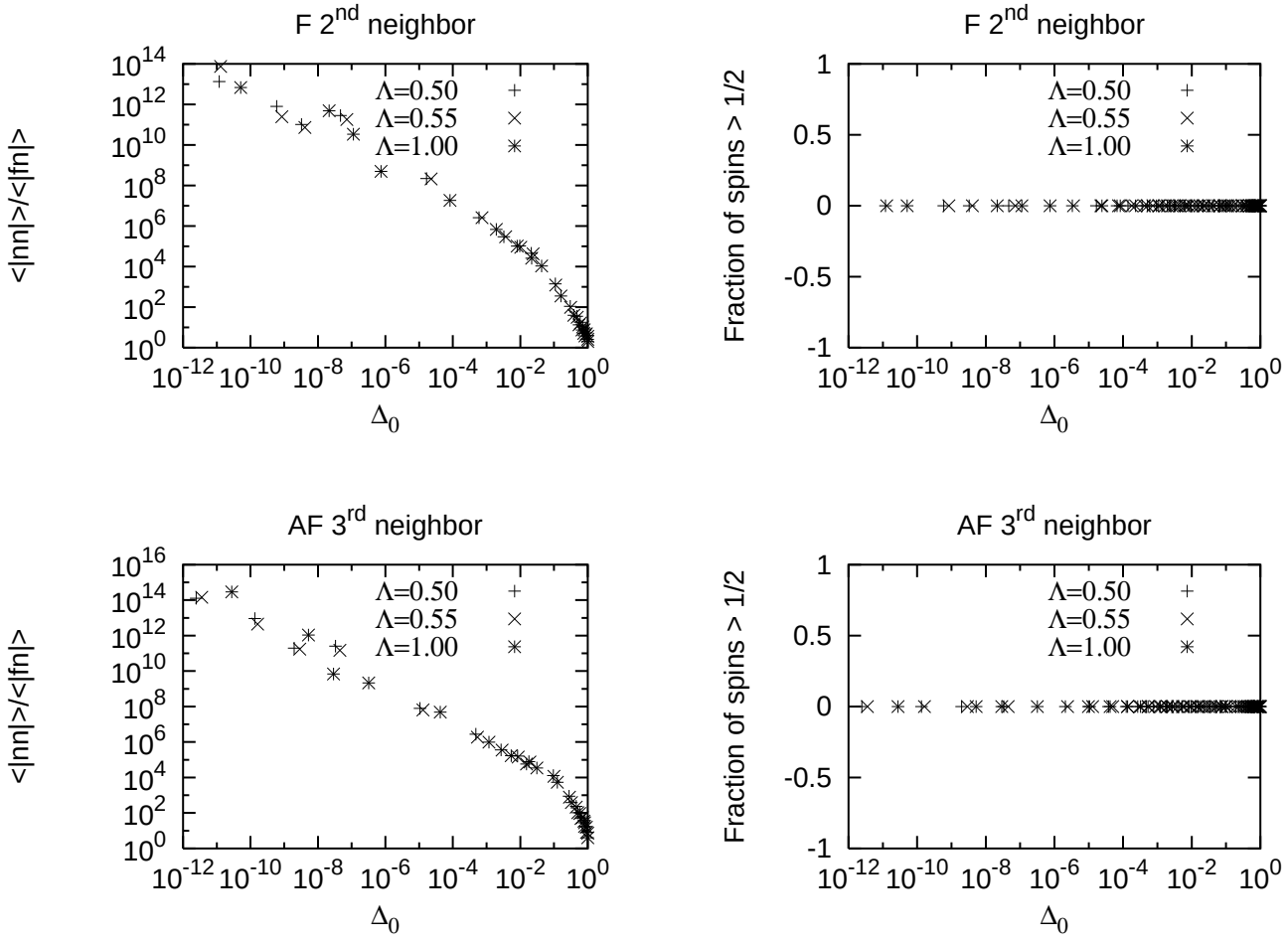

FIG. 7: The sample-averaged ratio of the strength of the nearest-neighbor bonds to the strength of the bonds that are beyond nearest neighbor and the fraction of spins larger than 1/2 as a function of energy scale as a function of energy scale for the model with no frustration introduced into the system. Two types of interactions which do not generate frustration, e.g. ferromagnetic second neighbors and antiferromagnetic third neighbors, are introduced into the system. The upper two panels show the calculation for a model in which ferromagnetic second-neighbor interactions are introduced into the system while the lower two panels for antiferromagnetic third-neighbor interactions. All graphs are calculated for $\alpha = 0$ but with varying Λ. It is clear from the plot that the interactions are dominated by nearest-neighbor bonds only regardless the value of Λ and there is no formation of effective spins whose sizes are larger than 1/2.